

Direct Observation of Enantiospecific Substitution in a Two-Dimensional Chiral Phase Transition

Bing Yang,[†] Yeliang Wang,[†] Huanyao Cun,[†] Shixuan Du,[†] Mingchun Xu,[†] Yue Wang,[‡] Karl-Heinz Ernst,^{§,*} and Hong-Jun Gao^{†,*}

Beijing National Laboratory of Condensed Matter Physics, Institute of Physics, Chinese Academy of Sciences, Beijing 100190, China, Key Lab of Supramolecular Structure and Materials, Jilin University, Changchun 130023, China, and Empa, Swiss Federal Laboratories for Materials Testing and Research, Überlandstrasse 129, CH-8600 Dübendorf, Switzerland

Received April 9, 2010; E-mail: h.j.gao@aphy.iphy.ac.cn; karl-heinz.ernst@empa.ch

Abstract: Initial stages of a chiral phase transition in the monolayer of a quinacridone derivative on the Au(111) surface were investigated by scanning tunneling microscopy at submolecular resolution. The prochiral molecules form a homochiral lamella phase at low coverages upon adsorption. A transition to a racemate lattice is observed with increasing coverage. Enantiomers of a homochiral lamella line become specifically substituted by opposite enantiomers such that a heterochiral structure evolves. Due to the higher density, lateral alkyl chains are bent away from the surface. Our findings are significant for the understanding and control of chiral phase transitions in related molecular systems like liquid crystals.

1. Introduction

When a racemic mixture of chiral molecules condenses it may form (i) a racemic compound, in which both enantiomers are present in the same single crystal; (ii) a conglomerate, in which the single crystals contain only one enantiomer, but the sample as a whole is racemic; and, quite rarely, (iii) a solid solution of both enantiomers.¹ There are still no satisfying explanations for the fact that some chiral compounds crystallize into conglomerates, but the vast majority do not.² Wallach provided in 1895 an explanation based on eight chiral compounds, stating that racemic lattices pack more densely than homochiral ones.³ Together with Kitajgorodskij's principle of close packing,⁴ this would explain the higher stability of racemic crystals. A thermodynamic argument for higher racemate stability has been brought forward as well,¹ but was proven to be fallacious.⁵ Brock et al. further showed that Wallach's rule is inconclusive in the general case and comes with a bias for the group of chiral compounds with resolvable enantiomers.⁵

Because of the complex situation in common crystallization, well-defined model systems are a good choice to gain insight at a microscopic level. This has been demonstrated in the field of heterogeneous catalysis, where details of surface reactions have been investigated on single-crystal surfaces in ultrahigh vacuum, i.e., far from the working conditions.⁶ The adsorption of chiral molecules on single crystal surfaces is also deployed

as an approach for better understanding the phenomenon of optical resolution of enantiomers.⁷ Chiral surface systems have potential applications in enantioselective heterogeneous catalysis,⁸ nonlinear optics,⁹ and liquid-crystal display technologies.¹⁰ Using scanning tunneling microscopy (STM), various chiral structures, like clusters,¹¹ filaments,¹² and two-dimensional (2D) domains,¹³ have been studied at the molecular scale. The phenomena addressed were chiral recognition,^{7,14} chirality amplification,¹⁵ and chiral switching.¹⁶ Moreover, it has been predicted that 2D enantiomeric resolution on a surface should occur more easily than in 3D crystals.¹⁷ Due to confinement in the plane certain symmetry elements, e.g. the center of inversion

- (7) (a) Ernst, K.-H. *Top. Curr. Chem.* **2006**, 265, 209. (b) Raval, R. *Chem. Soc. Rev.* **2009**, 38, 707. (c) Katsonis, N.; Lacaze, E.; Feringa, B. L. *J. Mater. Chem.* **2008**, 18, 2065.
- (8) (a) Zaera, F. *J. Phys. Chem. C* **2008**, 112, 16196. Bürgi, T.; Baiker, A. *Acc. Chem. Res.* **2004**, 37, 909. Yoon, T. P.; Jacobsen, E. N. *Science* **2003**, 299, 1691.
- (9) Verbiest, T.; Van Elshocht, S.; Kauranen, M.; Helleman, L.; Snauwaert, J.; Nuckolls, C. K., T. J.; Persoons, A. *Science* **1998**, 282, 913.
- (10) (a) Lemieux, R. P. *Acc. Chem. Res.* **2001**, 34, 845. (b) Barbera, J.; Giorgini, L.; Paris, F.; Salatelli, E.; Tejedor, R. M.; Angiolini, L. *Chem.-Eur. J.* **2008**, 14, 11209. (c) Lin, S. C.; Lin, T. F.; Ho, R. M.; Chang, C. Y.; Hsu, C. S. *Adv. Func. Mater.* **2008**, 18, 3386.
- (11) (a) Böhringer, M.; Morgenstern, K.; Schneider, W.-D.; Berndt, R.; Mauri, F.; Vita, A. D.; Car, R. *Phys. Rev. Lett.* **1999**, 83, 324. (b) Kühnle, A.; Linderoth, T. R.; Hammer, B.; Besenbacher, F. *Nature* **2002**, 415, 891. (c) Blüm, M. C.; Cavar, E.; Pivetta, M.; Patthey, F.; Schneider, W. D. *Angew. Chem., Int. Ed.* **2005**, 44, 5334. (d) Kühnle, A.; Linderoth, T. R.; Besenbacher, F. *J. Am. Chem. Soc.* **2003**, 125, 14680.
- (12) (a) Barth, J. V.; Weckesser, J.; Trimarchi, G.; Vladimirova, M.; Vita, A. D.; Cai, C.; Brune, H.; Günter, P.; Kern, K. *J. Am. Chem. Soc.* **2002**, 124, 7991. (b) Böhringer, M.; Schneider, W. D.; Berndt, R. *Angew. Chem., Int. Ed.* **2000**, 39, 792.
- (13) (a) Wei, Y. H.; Kannappan, K.; Flynn, G. W.; Zimmt, M. B. *J. Am. Chem. Soc.* **2004**, 126, 5318. (b) Fasel, R.; Parschau, M.; Ernst, K. H. *Angew. Chem., Int. Ed.* **2003**, 42, 5178. (c) Cai, Y.; Bernasek, S. L. *J. Phys. Chem. B.* **2005**, 109, 4514.
- (14) Rao, B. V.; Kwon, K. Y.; Zhang, J.; Liu, A. W.; Bartels, L. *Langmuir* **2004**, 20, 4406.

[†] Chinese Academy of Sciences.

[‡] Jilin University.

[§] Swiss Federal Laboratories for Materials Testing and Research.

- (1) Jacques, J.; Collet, A.; Wilen, S. H. *Enantiomers, Racemates and Resolutions*; Krieger Publishing Co.: Malabar, FL, 1994.
- (2) Pérez-García, L.; Amabilino, D. B. *Chem. Soc. Rev.* **2007**, 36, 941.
- (3) Wallach, O. *Liebigs Ann. Chem.* **1895**, 286, 90.
- (4) Kitajgorodskij, A. I. *Acta Crystallogr.* **1965**, 18, 585.
- (5) Brock, C. P.; Schweitzer, W. B.; Dunitz, J. D. *J. Am. Chem. Soc.* **1991**, 113, 9811.
- (6) Ertl, G. *Angew. Chem., Int. Ed.* **2008**, 47, 3524 (Nobel Lecture 2007).

or the glide plane parallel to the surface, are precluded and enhanced chiral interactions are expected.¹⁸ At surfaces, 2D chiral phase transitions, i.e., conversion from a conglomerate of two homochiral phases into one racemic phase, have been observed in monolayers of chiral and prochiral species.^{12b,19} However, previous work basically reported structural details before and after the transition and did not draw conclusions on the transformation process itself.

Here we report a chiral phase transition from a conglomerate of homochiral domains into a racemic close-packed structure with increasing coverage for *N,N'*-dihexadecylquinacridone ($C_{52}H_{76}O_2N_2$; QA16C) on the Au(111) surface. Quinacridone and its derivatives are well-known organic semiconductor materials that display excellent chemical stability²⁰ and are promising candidates for high-performance organic light-emitting devices.²¹ Besides the aromatic backbone, QA16C has two alkyl chains with 16 carbon atoms each. This combination of rigid backbone and flexible alkyl side chains makes QA16C an interesting model for understanding the intermolecular interactions in liquid crystal science. The molecules are prochiral in the gas or liquid phase, but become chiral due to 2D confinement at the surface. Therefore, QA16C molecules are distinguishable on the surface as right- and left-handed enantiomers, denoted here as R- and L-QA16C, respectively (Figure 1). In particular, the initial stages of the evolution of heterochirality from homochirality have been monitored by means of high-resolution STM. This allowed determination of the absolute configuration of single enantiomers and identification of enantioselective adsorption, i.e., only opposite-handed molecules are incorporated into the homochiral lattice.

2. Experimental Section

The experiments were carried out in an ultrahigh vacuum (UHV, $p = 2 \times 10^{-10}$ mbar) system, equipped with a variable-temperature STM (Omicron Nanotechnology). Before transfer into the UHV-chamber, the Au(111) crystal (MaTeck) was cleaned in an ultrasonic bath in acetone, ethanol, and water, in this sequence, three times. The clean Au(111) surface was finally obtained after several cycles of in vacuo argon ion sputtering followed by annealing at 750 K. Relatively wide terraces showing the herringbone reconstruction were observed by STM after this treatment. QA16C was purified

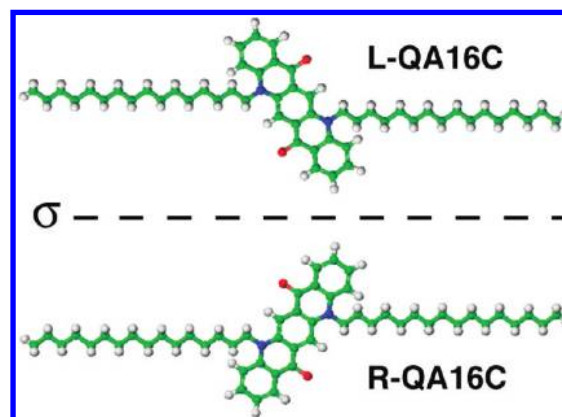


Figure 1. Molecular models of QA16C enantiomers at the surface.

by sublimation at low pressures ($p \approx 10^{-7}$ mbar), followed by degassing at 440 K for 2 h in UHV. QA16C was deposited onto the Au(111) substrate by means of organic molecular beam epitaxy at 460 K cell temperature. STM measurements were performed with a tungsten tip (prepared by electrochemically etching) at room temperature.

3. Results and Discussion

Figure 2 shows different chiral phases with increasing coverage. At coverages below 0.023 ML (1 ML is defined as 1.39×10^{19} molecules/m², corresponding to one molecule per Au(111) surface atom), a homochiral lamella structure is formed (Figure 2a). Similar motifs are known from self-assembly of long alkyl chain molecules at the liquid/graphite interface²² and for QA16C on Cu(110) and Ag(110).²³ The aromatic backbones as well as the alkyl chains are clearly distinguished as bright protrusions and dim stripes between the bright parallel rows, respectively. The entire QA16C adlayer is well-ordered. Two types of enantiomorphous domains (denoted as R and L) coexist on the surface (Supporting Information, Figure S1). Each domain consists of pure enantiomers of QA16C and is therefore a manifestation of homochirality. The shorter unit cell vector **a** of the (4 0, 3 11) unit cell is aligned parallel to the <110> directions,²⁴ whereby the molecular backbones are tilted by $\pm 45^\circ$ with respect to <110>. Structural details of the homochiral and racemic lattices are given in the Supporting Information. The close distance between adjacent molecular backbones allows strong intermolecular hydrogen bonds between the oxygen and hydrogen atoms of adjacent molecules (Supporting Information, Figure S2). The O \cdots H-C length is estimated to be 2 Å, which is in the range of the ideal hydrogen bond length.²⁵ The interdigitation of the long alkyl chains also favors the formation of this well-ordered architecture via lateral van der Waals interactions.²² However, that interdigitation is the driving force for homochiral domains is not certain. A hypothetical hetero-

- (15) (a) Fasel, R.; Parschau, M.; Ernst, K. H. *Nature* **2006**, *439*, 449. (b) Parschau, M.; Fasel, R.; Ernst, K.-H. *J. Cryst. Growth Des.* **2008**, *8*, 1890. (c) Haq, S.; Liu, N.; Humboldt, V.; Jansen, A. P. J.; Raval, R. *Nat. Chem.* **2009**, *1*, 409. (d) Parschau, M.; Romer, S.; Ernst, K.-H. *J. Am. Chem. Soc.* **2004**, *126*, 15398. (e) Parschau, M.; Kampen, T.; Ernst, K.-H. *Chem. Phys. Lett.* **2005**, *407*, 433.
- (16) (a) Weigelt, S.; Busse, C.; Petersen, L.; Rauls, E.; Hammer, B.; Gothelf, K. V.; Besenbacher, F.; Linderoth, T. R. *Nat. Mater.* **2006**, *5*, 112. (b) Busse, C.; Weigelt, S.; Petersen, L.; Laegsgaard, E.; Besenbacher, F.; Linderoth, T. R.; Thomsen, A. H.; Nielsen, M.; Gothelf, K. V. *J. Phys. Chem. B* **2007**, *111*, 5850.
- (17) Arnett, E. M.; Chao, J.; Kinzig, B.; Stewart, M. V.; Thompson, O.; Verbiar, R. J. *J. Am. Chem. Soc.* **1982**, *104*, 389.
- (18) Lahav, M.; Leiserowitz, L. *Angew. Chem., Int. Ed.* **1999**, *38*, 2533.
- (19) (a) Behzadi, B.; Romer, S.; Fasel, R.; Ernst, K. H. *J. Am. Chem. Soc.* **2004**, *126*, 9176. (b) Romer, S.; Behzadi, B.; Fasel, R.; Ernst, K. H. *Chem.—Eur. J.* **2005**, *11*, 4149. (c) Vidal, F.; Delvigne, E.; Stepanow, S.; Lin, N.; Barth, J. V.; Kern, K. *J. Am. Chem. Soc.* **2005**, *127*, 10101. (d) Stepanow, S.; Lin, N.; Vidal, F.; Landa, A.; Ruben, M.; Barth, J. V.; Kern, K. *Nano Lett.* **2005**, *5*, 901.
- (20) Ye, K.; Wang, J.; Sun, H.; Liu, Y.; Mu, Z.; Li, F.; Jiang, S.; Zhang, J.; Zhang, H.; Wang, Y.; Che, C.-M. *J. Phys. Chem. B* **2005**, *109*, 8008. (b) Wang, J.; Zhao, Y.; Zhang, J.; Zhang, J.; Yang, B.; Wang, Y.; Zhang, D.; You, H.; Ma, D. *J. Phys. Chem. C* **2007**, *111*, 9177.
- (21) Gross, E. M.; Anderson, J. D.; Slaterbeck, A. F.; Thayumanavan, S.; Barlow, S.; Zhang, Y.; Marder, S. R.; Hall, H. K.; Nabor, M. F.; Wang, J. F.; Mash, E. A.; Armstrong, N. R.; Wightman, R. M. *J. Am. Chem. Soc.* **2000**, *122*, 4972.
- (22) De Feyter, S.; De Schryver, F. *J. Phys. Chem. B* **2005**, *109*, 4290.
- (23) (a) Yang, X.; Wang, J.; Zhang, X.; Wang, Z.; Wang, Y. *Langmuir* **2007**, *23*, 1287. (b) Lin, F.; Zhong, D. Y.; Chi, L. F.; Ye, K.; Wang, Y.; Fuchs, H. *Phys. Rev. B* **2006**, *73*, 235420. (c) Shi, D.; Ji, W.; Lin, X.; He, X.; Lian, J.; Gao, L.; Cai, J.; Lin, H.; Du, S.; Lin, F.; Seidel, C.; Chi, L.; Hofer, W.; Fuchs, H.; Gao, H. *J. Phys. Rev. Lett.* **2006**, *96*, 226101. (d) Cun, H.; Wang, Y.; Yang, B.; Du, S.; Wang, Y.; Ernst, K.-H.; Gao, H. *J. Langmuir* **2010**, *26*, 3402.
- (24) (a) $(m_1 m_2, m_2 m_2)$ links the adsorbate lattice vectors (**a**, **b**) to the substrate lattice vectors (**a_S**, **b_S**) via $\mathbf{a} = m_1 \mathbf{a}_S + m_2 \mathbf{b}_S$ and $\mathbf{b} = m_2 \mathbf{a}_S + m_2 \mathbf{b}_S$. Park, R. L.; Madden, H. H. *Surf. Sci.* **1968**, *11*, 188. (b) Rules for the correct choice for the unit cell vectors have been defined recently: Merz, L.; Ernst, K.-H. *Surf. Sci.* **2010**, *604*, 1049.
- (25) Barbosa, L. A. M. M.; Sautet, P. *J. Am. Chem. Soc.* **2001**, *123*, 6639.

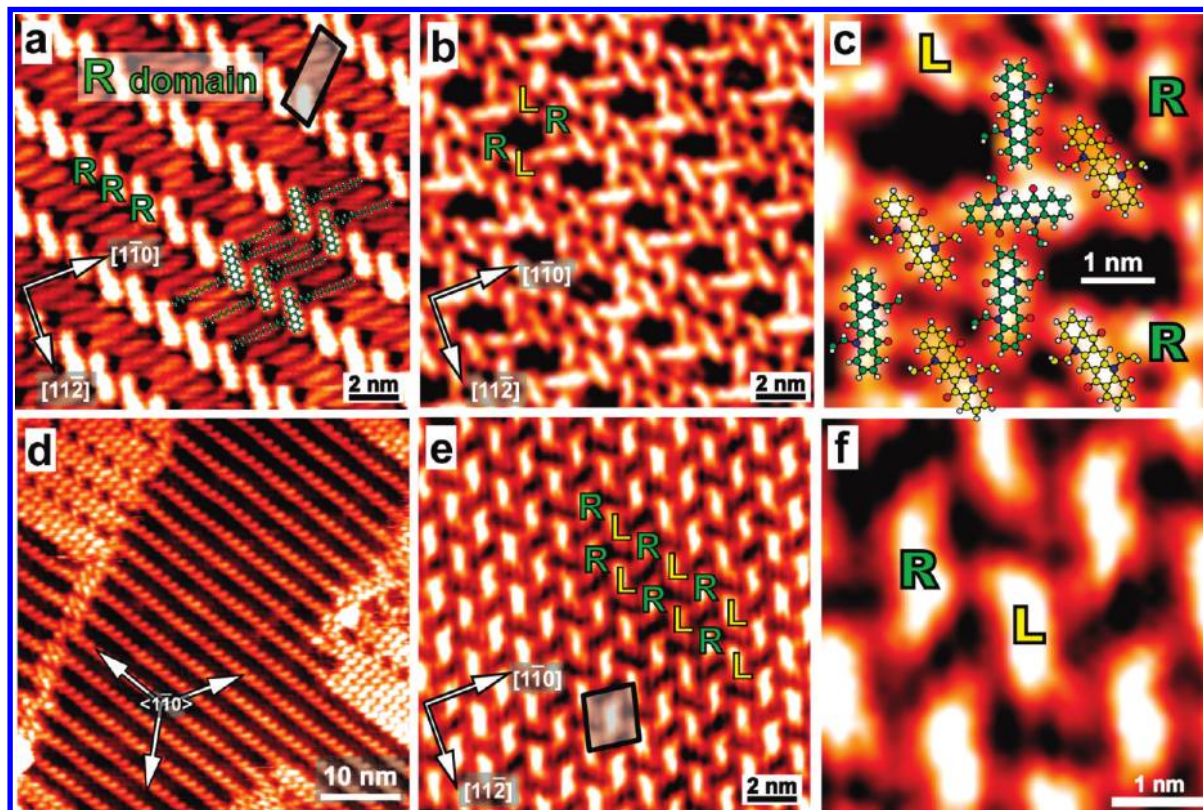


Figure 2. STM images of QA16C molecules on Au(111) for different coverages. (a) Homochiral R-lamella structure at 0.023 ML. (b) Intermediate heterochiral phase, $\theta = 0.052$ ML. (c) Detail from part b, superimposed with aromatic backbones of the molecules and assignment of the handedness. (d) Coexistence of lamella and intermediate structures, $\theta = 0.026$ ML. The equivalent $\langle 1\bar{1}0 \rangle$ directions are identified. (e) Racemic saturation structure, $\theta = 0.062$ ML. (f) High-resolution image of racemic structure with R- and L-enantiomer assignment. The unit cells are indicated in parts a and e. Tunneling parameters for parts a–c, e, f, $U = 1.1$ V, $I = 0.08$ nA; tunneling parameters for part d, $U = 1.2$ V, $I = 0.09$ nA.

chiral structure at this coverage may allow interdigititation of the alkyl chains as well, even with the backbones at opposite tilt angles in every second line. An example for such heterochiral lamella structure is a bis-thiaalkyanthracene derivative on graphite.^{13a}

With increasing coverage, a heterochiral intermediate phase (Figures 2b–d) and a racemic close-packed structure (Figures 2e,f) are observed. The additional molecules adsorb into the spacing between the QA16C backbone lamella structure rows, leading to the intermediate phase with close-packed racemic double rows and loose-packed homochiral rows (Figure 2b). The loose-packed row molecules still have the handedness from the original phase but are oriented normal to the alignment in the lamella phase (Figure 2c). The ratio of close-packed to loose-packed molecules further increases with coverage, until finally at 0.062 ML the intermediate phase has fully disappeared into the racemic close-packed structure (Figure 2e). This means for a single domain that the enantiomeric excess decreases gradually, but the distribution is not random! Long-range STM images of this transition process are presented in the Supporting Information (Figure S3). This is a rare example of a lattice with enantiomeric excess, but not being a solid solution. The few previous studies of enantiomeric excess systems at surfaces rather suppress one of the originally observed two enantiomers and form in addition a solid solution containing an unbalanced mix of the enantiomers.^{15a–c}

The alkyl chains of QA16C molecules are not resolved by STM in the close-packed structure. We assign this to a partial uplift of the alkyl chains away from the surface. A similar case

has been reported only for the solid–liquid interface so far.²⁶ Assuming that the chains are flexible and are allowed to occupy different configurations, such a process would increase entropy. The side-chain orientation does not have to be necessarily normal to the surface. Their disappearance in STM can be explained by alignment on top of adjacent molecule backbones in combination with the different STM contrast for the aliphatic and aromatic part. In order to prove that the molecular chains are still connected to the backbone, however, we induced desorption of a fraction of the monolayer by heating the sample to 580 K. After this treatment the reappearance of the lamella structure was observed at room temperature (Supporting Information, Figure S4). Even without imaging lateral extended aliphatic chains, the handedness of the adsorbates can be clearly distinguished (Figure 2c,f). R-QA16C has an ‘S-shape’, while L-QA16C displays the corresponding mirror image. On the basis of calculations, the enantiomorphous STM appearance of the aromatic QA backbone has previously been ascribed to the fact that the density of electronic states is higher at the oxygen.^{23a} Discrimination of the enantiomers in the close-packed structure clearly indicates the presence of a racemic lattice (Figure 2d).

The increase of total adsorption energy with increasing coverage is the driving force for the rearrangement from the lamella phase to the close-packed racemate structure. At low coverage the aromatic core–substrate, the chain–substrate, and the chain–chain interactions stabilize the interdigitated structure.

(26) De Feyter, S.; Larsson, M.; Gesquière, A.; Verheyen, H.; Louwet, F.; Groenendaal, B.; van Esch, J.; Feringa, B. L.; De Schryver, F. *ChemPhysChem*. **2002**, *11*, 966.

Since the chains are lifted off during the transition, the gain in adsorption energy must be mainly mediated by aromatic core–substrate interactions. The detachment of the alkyl chains from the metal substrate imposes an activation barrier on this process. We calculated a binding energy for a single hexadecane molecule on Au(111) of 67 kJ/mol (Supporting Information). This value serves as a rough estimate for the lift-off activation barrier, but ignores attractive chain–chain interaction due to interdigitation and could be therefore an underestimate. Values derived from thermal desorption of alkanes on various surfaces or physisorption of alkane thiolate on gold lie between 67 and 150 kJ/mol for alkyl chains or alkenes with 10–16 carbon atoms.²⁷ On Cu(110), for example, the QA16C monolayer does not show this phase transition and forms only the interdigitated homochiral lattice up to monolayer saturation.^{23d} Different outcome on different surfaces does not automatically identify the molecule–substrate interaction as the mechanism, since different structures include different lateral molecular interactions. A weaker molecule–substrate interaction also allows intermolecular recognition to come better into play. The balance of both intermolecular forces and molecule–substrate interaction may even allow coexistence of homochiral and racemic phases.²⁸ For Cu(110) and Au(111), however, both lamella structures are almost identical in structure and density. We therefore conclude that the extent of alkyl chain–substrate interaction makes the difference and does not allow a denser racemic structure on Cu(110). But this explains only homochiral recognition at low saturation coverage and the missing transition on Cu(110). Once the alkyl chains are detached, the system still has in principle the choice between hetero- and homochiral packing.

In order to understand why the heterochiral structure is favored at higher coverages, ab initio calculations for two model structures have been performed (see Supporting Information for details). We compared the adsorption energy of the observed racemic motif with a hypothetical homochiral arrangement of the same density. Due to computational limitations, we only considered side chains with two carbon atoms, which is justified by the fact that the long chains are not interacting with the metal surface. Figure 3 shows the two optimized lowest energy configurations for homochiral and racemic lattices. Our calculation clearly favors the heterochiral arrangement. The binding energy is about 284 meV/molecule higher than that of the homochiral arrangement. Even for the C2 alkyl chain derivative, our calculations favor the “bent-away” configuration for the alkyl chain. The racemate lattice in Figure 3 shows an interesting detail, that is, both enantiomers are not exactly located on identical substrate sites. Therefore, the adsorbates are not mirror images anymore and we actually deal with a 2D quasiracemate. A quasiracemate, due to different alignment in space of both enantiomers has been reported before.²⁹ In the present case, however, the molecular layer itself is truly racemic, but considering the adsorbate, i.e., molecule plus substrate, it is only quasiracemic. Consequently, mirror domains exist for the

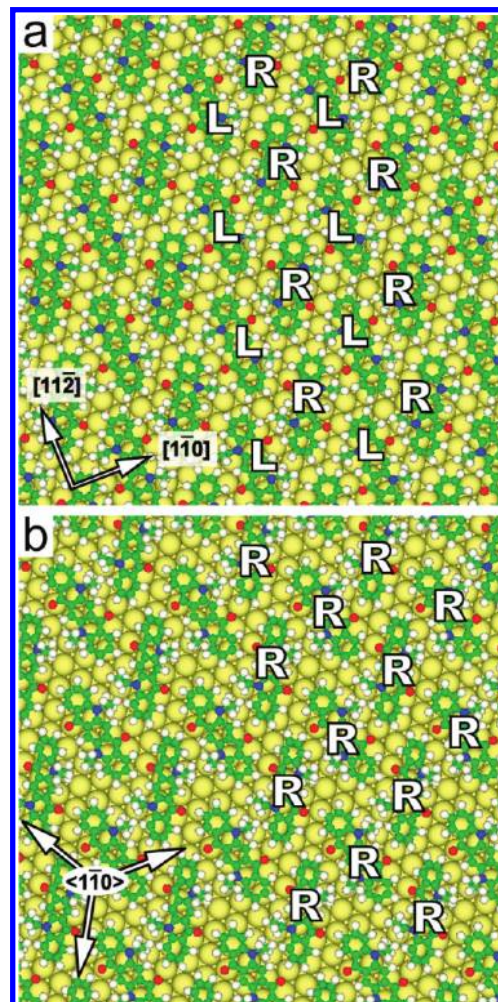


Figure 3. Optimized molecular model structures of close-packed layers with a heterochiral arrangement (a), as observed in the experiment, and a possible homochiral arrangement (b). High-symmetry surface directions are indicated.

racemic lattice as well, in which opposite enantiomers occupy the opposite surface sites in their unit cells.

For Langmuir–Blodgett films, stronger directed forces like hydrogen bonding have been predicted favoring chiral discrimination and conglomerate formation.³⁰ For both model structures shown in Figure 3, however, neither specific interactions between the molecular backbones and the metal surface nor differences in lateral interactions between homochiral and heterochiral molecular pairs are identified. This leaves us steric constraint in these close-packed structures. In the case of the hypothetical enantiopure structure of Figure 3b, the methylene groups of the two alkyl chains direct at the aromatic backbone are very close to each other, so that repulsion is strong. A higher repulsion lowers the maximum gain of the heat of adsorption and will actually lead to lower saturation coverage.

Hints to the nature of the chiral transition at microscopic level come from STM images taken at coverages just above 0.025 ML, i.e., from a supersaturated homochiral lamella structure that shows in part the intermediate phase (Figure 2d). All molecular overlayers shown in Figure 2 have densely packed rows along $\langle\bar{1}0\rangle$. During the phase transition with increasing coverage, the density increase is unidirectional, i.e., perpen-

(27) (a) Baxter, R. J.; Teobaldi, G.; Francesco, Z. *Langmuir* **2003**, *19*, 7335. (b) Lavrich, D. J.; Wetterer, S. M.; Bernasek, S. L.; Scoles, G. *J. Phys. Chem. B* **1998**, *102*, 3456. (c) Gellman, A. J.; Paserba, K. R. *J. Phys. Chem. B* **2002**, *106*, 13231. (d) Tait, S. L.; Dohnálek, Z.; Campbell, C. T.; Kay, B. D. *J. Chem. Phys.* **2006**, *125*, 234308.

(28) (a) Mamdouh, W.; Dong, M. D.; Kelly, R.; Kantorovich, L. N.; Besenbacher, F. *J. Phys. Chem. B* **2007**, *111*, 12048. (b) Cortes, R.; Mascaraque, A.; Schmidt-Weber, P.; Dil, H.; Kampen, T. U.; Horn, K. *Nano Lett.* **2008**, *8*, 4162.

(29) Cai, Y.; Bernasek, S. L. *J. Am. Chem. Soc.* **2003**, *125*, 1655.

(30) Andelman, D. *J. Am. Chem. Soc.* **1989**, *111*, 6536.

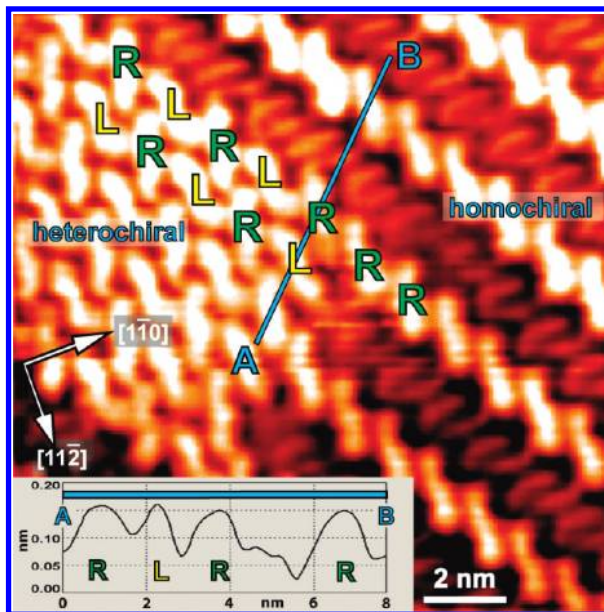


Figure 4. STM image of the initial stage of the transition at a phase boundary; $U = 1.1$ V, $I = 0.08$ nA. The inset shows the line profile corresponding to the blue line from A to B in the image. It illustrates the same height of the molecular backbone for all adsorbed molecules.

dicular to the rows. Instead of homochiral rows along $\langle 1\bar{1}0 \rangle$, rows with alternating handedness are observed. The enantiomer that has become replaced by the new opposite enantiomer is located next to the heterochiral line (Figure 2c), thus forming the above-mentioned homochiral loose-packed line. Consequently, the heterochiral lines run in the same direction as the homochiral lines (Figure 2d). Under these conditions, patches of the heterochiral close-packed structure are also formed at dislocations and domain boundaries (Figure 4). Although with no intermediate structure present, the scenario of the chiral phase transition is identical. Additional QA16C molecules adsorb into the homochiral domain and push the alkyl chains off the substrate in order to anchor directly on the substrate. This additional adsorption into the homochiral phase is an example of chiral recognition: Only molecules facing with the opposite enantiotopic side to the substrate than those of the homochiral phase underneath are allowed to become included. The alternative mechanism, where molecules are flipped in the adsorbed state, is excluded here due to the strong affinity between the QA16C backbone and the substrate. This would impose a much

higher barrier than directing molecules in a precursor adsorbate state into the favored chiral low-energy alignment. Our STM results reveal that within the close-packed molecular row, every second molecule is substituted and moves to the side. In Figure 4, for example, the substituted R-QA16C is repelled from the row and moves to a neighboring stable adsorption site, while an L-QA16C molecule occupies the original site. This process must induce the lift-off of the alkyl chains. A new heterochiral row is established from the laterally moved R-enantiomer and new adsorbing molecules, again directed into the L-alignment.

4. Conclusions

In conclusion, a chiral phase transition of QA16C molecules on the Au(111) surface has been investigated by STM in ultrahigh vacuum. At low coverage, only homochiral structures are observed. A denser packing with increasing coverage is only achieved due to detachment of the aliphatic side chains from the surface. After transition through an intermediate phase of local enantiomeric excess, a fully developed racemic lattice is formed. In particular, two steps have been identified in this chiral phase transition, that is, chiral recognition during additional adsorption and enantiospecific substitution of every second molecule in otherwise homochiral rows. The racemic lattice of QA16C on Au(111) packs more densely than a hypothetical homochiral saturation structure and is therefore an example for Wallach's rule in two dimensions. In contrast to the proposition that enantiomeric separation is more common in monomolecular layers, our example shows that this also depends on lateral density at the surface and that close packing can favor racemic crystals in two dimensions as well.

Acknowledgment. We thank J. D. Dunitz, K.-H. Rieder, and W. Ji for fruitful discussions and X. B. He for technical assistance. The work has been supported by NSFC, '863' and '973' projects, as well as the Shanghai Supercomputer Center in China. K.H.E. thanks the Swiss National Science Foundation (SNF) for support.

Supporting Information Available: STM images of mirror and rotational domain boundaries, structure model for the lamella phase, long-range STM images of all phases, unit cell parameters of the homochiral and racemic structures, STM images after annealing, as well as ab initio and MM+ calculation details. This material is available free of charge via the Internet at <http://pubs.acs.org>.

JA102989Y